

Elastic precursor effects during the $\text{Ba}_{1-x}\text{Sr}_x\text{TiO}_3$ ferroelastic phase transitions

Francesco Cordero,¹ Francesco Trequattrini,² Paulo Sergio da Silva Jr.,³ Michel Venet,³ Oktay Aktas,⁴ and Ekhard K. H. Salje⁵

¹*Istituto di Struttura della Materia-CNR (ISM-CNR), Area della Ricerca di Roma - Tor Vergata, Via del Fosso del Cavaliere 100, I-00133 Roma, Italy**

²*Dipartimento di Fisica, Università di Roma "La Sapienza", p.le A. Moro 2, I-00185 Roma, Italy*

³*Department of Physics, Federal University of São Carlos, 13565-905 São Carlos (SP), Brazil*

⁴*State Key Laboratory for Mechanical Behavior of Materials & School of Materials Science and Engineering, Xi'an Jiaotong University, Xi'an 710049, China*

⁵*Department of Earth Sciences, University of Cambridge, Downing Street, Cambridge CB2 3EQ, UK*

(Dated: December 23, 2022)

Elastic softening in the paraelastic phases of $\text{Ba}_{1-x}\text{Sr}_x\text{TiO}_3$ is largest near the transition temperatures and decreases on heating smoothly over extended temperature ranges. Softening extends to the highest measured temperature (850 K) for Ba-rich compounds. The temperature evolution of the excess compliance of the precursor softening follows a power law $\delta S \propto |T - T_C|^{-\kappa}$ with a characteristic exponent κ ranging between 1.5 in SrTiO_3 and 0.2 in BaTiO_3 . The latter value is below the estimated lower bounds of displacive systems with three orthogonal soft phonon branches (0.5). An alternative Vogel-Fulcher analysis shows that the softening is described by extremely low Vogel-Fulcher energies E_a , which increase from SrTiO_3 to BaTiO_3 indicating a change from a displacive to a weakly order/disorder character of the elastic precursor. Mixed crystals of $\text{Ba}_x\text{Sr}_{1-x}\text{TiO}_3$ possess intermediate behaviour. The amplitudes of the precursor elastic softening increases continuously from SrTiO_3 to BaTiO_3 . Using power law fittings reveals that the elastic softening is still 33% of the unsoftened Young's modulus at temperatures as high as 750 K in BaTiO_3 with $\kappa \simeq 0.2$. This proves that the high temperature elastic properties of these materials are drastically affected by elastic precursor softening.

I. INTRODUCTION

Ferroelastic materials [1] commonly display large elastic anomalies during structural phase transitions [2]. Structural collapses can lead to a total reduction of the effective moduli in case of proper ferroelastics like in BiVO_4 and LaNbO_3 [3–5]. In the case of improper ferroelastics, like ferroelectric BaTiO_3 and antiferrodistortive SrTiO_3 , a direct coupling between the acoustic [6] soft mode and the elastic moduli is symmetry forbidden while typical elastic softening still reduces the moduli by some 20–50% [7]. In ferroelectrics, the intrinsic softening of the low-temperature phase with respect to the paraelectric phase is due to the combined direct and converse piezoelectric effects [8, 9]. Additional softening in the low temperature phases may be due to mobile twin boundaries just below but close to the transition point, which vanishes if the twin walls are strongly pinned [10–12]. Thick domain walls were shown to be less prone to such pinning effects [13–15] and many examples of highly mobile wall movements during the softening process have been reported [16–21]. We argue in this paper that significant precursor softening is commonly observed in the paraelastic phase which can be – in some cases – directly related to intrinsic disorder of the high temperature phase and dynamic local nano-structures. Conceptually, this effect is best observed when materials are disordered by extrinsic forces such as radioactive bombardment. Consider a single crystal without any domain boundaries which is then disordered by the radioactive decay of radiogenic impurities. Such samples will massively reduce their elastic moduli due to the structural heterogeneity. This situation is often encountered in so-called metamict materials such as zircon [22] and

titanite [23] where the reduction in bulk and shear modulus is greater than 50%, while their structure is still unchanged. Structural disorder of the paraelastic phase and significant short-range order is, thus, expected if the ferroelastic phase transition is of the order-disorder type and structural variations occur in nominally cubic materials [24–28].

Displacive systems show similar effects although to a lesser extent [29]. Following the initial theoretical analysis of Pytte [30, 31] and Axe & Shirane [32], fluctuation contributions to elastic softening have usually been considered in terms of coupling between different vibrational modes [33–38]. In both cases local fluctuations with high local correlations can be expected. Typical examples for local nano-structures are tweed structures with interwoven, dynamical strain fields. They were found by molecular dynamics simulations and diffractions experiments [39–42]. Similar effects were postulated by Pelc *et al.* [43] for high temperature superconductors.

The underlying physical picture for displacive precursor softening is that, associated with a soft mode at some specific point in reciprocal space, there will be a set of branches which also soften to some extent. Along with the soft mode itself, when the frequencies of modes along the soft branches decrease, their amplitudes become larger and they can combine to produce stress fluctuations and associated strain fluctuations. The summation of all such combinations will yield a net softening of some specific acoustic modes depending on the dimensionality of the elastic softening [2]. The total effect increases as the amplitudes of the modes increase, reaching a maximum at the transition point. The detailed temperature dependence is usually uncertain because it requires an exact knowledge of mode mixing properties [44], including potential local modes which are not captured by conventional spectroscopy. Nevertheless, it was advocated that the resulting temperature dependence of the elastic softening can be

* [francesco.cordero@ism.cnr.it]

described conveniently by a power law [2, 29, 45]:

$$\Delta C_{ik} = A_{ik}(T - T_c)^\kappa. \quad (1)$$

A_{ik} and κ are properties of the material of interest. The temperature T_c is below the transition temperature T_{tr} . Such power laws are inspired by simple soft-mode mechanisms, although κ is sensitive to the details of mode-mode coupling, the degree of anisotropy of dispersion curves about the reciprocal lattice vector of the soft mode, and to the extent of softening along each branch. This effect mimics the bilinear coupling between the order parameter and strain. In the most common case, where direct interactions are symmetry forbidden, there are still mechanisms which lead to softening in the displacive limit. For example, optical phonons with opposite wavevectors \mathbf{q} and $-\mathbf{q}$ can combine to produce a fluctuating strain field. The symmetry allowed coupling is $e_{\text{local}} \langle Q^2 \rangle$, where e_{local} is the local strain field and $\langle Q^2 \rangle$ is the average two-phonon amplitude.

Alternatively, when local disorder leads to thermally activated dynamics with a broad distribution of activation energies and a threshold related to the phase transition temperature, the elastic softening may follow a Vogel-Fulcher statistics [46, 47] with

$$\Delta C_{ik} = B_{ik} \exp\left(\frac{E_a/k_B}{T - T_{VF}}\right), \quad (2)$$

where B_{ik} is a materials parameter, E_a the activation energy and T_{VF} is the Vogel-Fulcher energy [47–49]. Even though Eq. (2) is not the result of a formal theory, such behaviour is typical for glasses and for local clusters in order-disorder phase transitions. In $\text{Ba}_{1-x}\text{Sr}_x\text{TiO}_3$ the two archetypal softening mechanisms, namely the displacive power law and a mixed order-disorder Vogel-Fulcher mechanism can be expected to be related to the antiferrodistortive displacive transition in SrTiO_3 at 105.6 K [50] and the ferroelectric/ferroelastic transition in BaTiO_3 at 400 K, which contains aspects of disorder from Ti off-centering in the paraelectric phase [51–53].

In materials investigated in this study the elastic precursor softening [2, 54, 55] is significant, including complex intermediate cases [56, 57]. The power law softening and, to a lesser extent, the Vogel-Fulcher softening describe the experimental observations very well over a wide temperature range. The two limiting cases, SrTiO_3 and BaTiO_3 , behave very differently, and a smooth variation of the model parameters A , κ , B , E_a is indeed observed in mixed crystals $\text{Ba}_{1-x}\text{Sr}_x\text{TiO}_3$ as function of the chemical composition.

II. SAMPLE PREPARATION

Ceramic $\text{Ba}_{1-x}\text{Sr}_x\text{TiO}_3$ samples were prepared in two different laboratories with different solid state sintering procedures. The BaTiO_3 sample is BT #1 of Ref. [58], prepared from commercial high purity powder of BaTiO_3 (99.9%, Sigma-Aldrich). The powder was first heated at 800 K for 2 h to remove undesired organics and ball milled for 24 h in order

x(Sr)	Density (g/cm ³)	Relative density (%)
0	5.64	93.7
0.03	5.85	97.5
0.1	5.83	97.9
0.3	5.67	97.8
0.5	5.35	95.9
1	5.02	97.9

TABLE I. Density of ceramic samples $\text{Ba}_{1-x}\text{Sr}_x\text{TiO}_3$, assuming a linear theoretical density that changes linearly between 5.13 g/cm³ of SrTiO_3 and 6.02 g/cm³ of BaTiO_3 .

to reduce and homogenise the distribution of particle sizes. It was then mixed with 3 wt.% polyvinyl butyral (PVB) as a binder, uniaxially pressed at 150 MPa into a thick bar, isostatically pressed at 250 MPa, and sintered at 1350 °C for 2 h. The $\text{Ba}_{1-x}\text{Sr}_x\text{TiO}_3$ materials were synthesized starting from high-purity powders of BaCO_3 (99.8%, Alfa Aesar), SrCO_3 (98%, Merck), and TiO_2 (99.8%, Merck) mixed for 24 h and then calcined at 1150 °C for 5 h. The calcined BST powders were checked by XRD to be perovskite tetragonal ($P4mm$) phase, milled for 24 h to obtain a homogeneous particle size distribution around 1 μm , and mixed with 3 wt.% polyvinyl butyral (PVB) as a binder. Bar ingots were uniaxially pressed at 190 MPa into metallic molds, isostatically pressed at 250 MPa and conventionally sintered at 1350 °C for 4 h. All samples were checked by XRD and their densities are listed in Table I. The resulting ceramics were cut into thin bars with lengths of 35–42 mm, widths of 4–6 mm and thicknesses of 0.4–0.7 mm, mechanically polished and annealed at 750 °C for 2 h to release stresses.

The SrTiO_3 sample was prepared by solid-state reaction of SrCO_3 (Aldrich, 99.9%) and TiO_2 (Aldrich, 99.9%) for 6 h at 1100 °C. The resulting powder was milled, sieved and pressed in a bar and sintered in air at 1450 °C for 24 h. Thin bars 43 mm long and 0.5 mm thick were cut and polished for the anelastic measurements. The $\text{Ba}_{0.5}\text{Sr}_{0.5}\text{TiO}_3$ bar, 37 mm long and 0.44 mm thick, was prepared in a similar manner. The sample of SrTiO_3 had $T_{tr} \simeq 111$ K, which is 5.3 K above the value generally found. A possible explanation is a larger than usual content of Ca impurities in the starting SrCO_3 powder. To avoid artifacts due to impurities, we also used a single crystal of SrTiO_3 with dimensions of 26.15 3.4 0.5 mm³, cut from a wafer of M.T.I. Corporation with the edges parallel to the $\langle 100 \rangle$ directions.

III. EXPERIMENTAL METHODS

The dynamic Young's modulus E was measured by electrostatically exciting the free flexural modes of the bars suspended in vacuum on thin thermocouple wires, as described in Ref. [59]. The real part is deduced from the resonant frequency of the fundamental flexural mode [60]

$$f = 1.028 \frac{t}{l^2} \sqrt{\frac{E}{\rho}}. \quad (3)$$

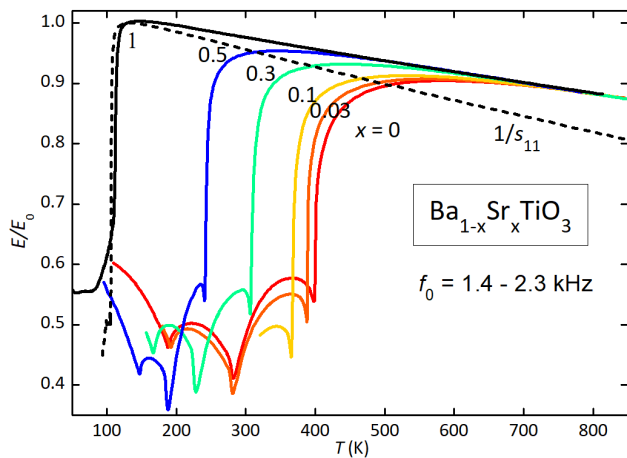


FIG. 1. Young's moduli of $\text{Ba}_{1-x}\text{Sr}_x\text{TiO}_3$ ceramics normalized to overlap at $T \gg T_C$. The dashed line is $1/s_{11}$ of the SrTiO_3 crystal.

For the $\langle 100 \rangle$ oriented crystal of SrTiO_3 we measured $E = s_{11}^{-1}$. We do not consider the absolute values of the Young's moduli, but their normalized values, $E(T)/E_0 = (f(T)/f_0)^2$, where the temperature dependence of the density in Eq. (3) is ignored in comparison with the elastic moduli. Its linear dependence does not influence the fits, since it is absorbed in the fit of the background elastic modulus.

IV. RESULTS

Fig. 1 presents the Young's moduli of $\text{Ba}_{1-x}\text{Sr}_x\text{TiO}_3$ normalized to overlap at high temperature. The purpose of this figure is to show that the anharmonic linear softening (*i.e.* the slope dE/dT) is similar for all compositions. The slope of the single crystal is different because the Young's modulus of a ceramic cubic material is

$$E^{-1} = S_{11} - \frac{2}{5} \left(S_{11} - S_{12} - \frac{1}{2} S_{44} \right), \quad (4)$$

while that of a $\langle 100 \rangle$ oriented crystal is $E^{-1} = S_{11}$ [60], and the various S_{ij} may have different slopes.

The measurement of BaTiO_3 was already reported in Ref. [58] (Fig. 1, sample BT #1). In addition to the step at the transition from the cubic paraelectric to the tetragonal ferroelectric phases, there are two additional minima due to the ferroelectric transitions to the orthorhombic and rhombohedral phases. In SrTiO_3 the structural transition is antiferrodistortive, with tilting of the TiO_6 octahedra around the c axis. A changeover of the character of the structural transitions in $\text{Ba}_{1-x}\text{Sr}_x\text{TiO}_3$ was projected at $x \approx 0.8-0.9$ [61]. The normalization of E in Fig. 1 only shows that the temperature slopes in the high temperature limits of $E(T)$ coincide even though the absolute values of the moduli are different. These absolute moduli are difficult to compare with each other due to irregularities in the sample shapes and differences in porosity, which are not included in Eq. (3) but reduce E in manners

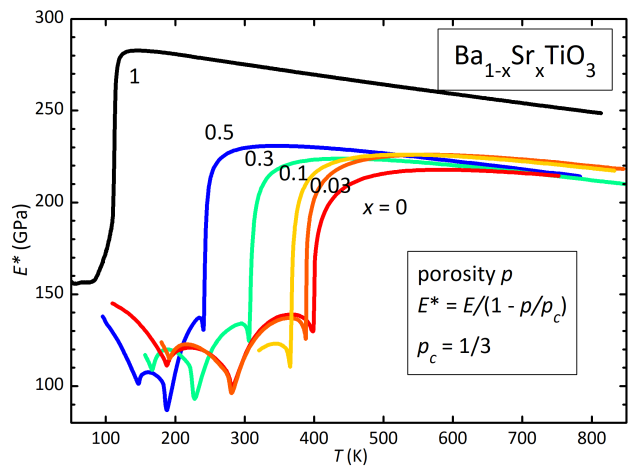


FIG. 2. Young's moduli of $\text{Ba}_{1-x}\text{Sr}_x\text{TiO}_3$ corrected for porosity of the ceramic samples.

that depend on the amount and type of porosity [62–64]. We corrected for porosity effects using the linear decrease in the Young's modulus [62],

$$E = E^*(1 - p/p_c), \quad (5)$$

where E is the measured modulus, E^* the modulus of the dense material and p_c is a critical porosity. We chose $p_c = 1/3$ because it yields 218 GPa for the maximum value reached by BaTiO_3 in the PE phase, in good agreement with 214 GPa for the single crystal [64, 65], and 275 GPa for the room temperature value of SrTiO_3 , in agreement with 285 GPa of Ref. [66]. The result is shown in Fig. 2.

The modulus of the paraelastic phase of $\text{Ba}_{1-x}\text{Sr}_x\text{TiO}_3$ increases with x , though the $x = 0.3$ and 0.5 compositions are well below a linear trend. This may be an artifact because the relative density measured by the Archimedes method underestimates the open porosity, and strong deviations from a simple formula like Eq. (5) may occur, as shown for BaTiO_3 [64].

We show in Fig. 3 the data normalized both in magnitude with respect to the maximum value of the modulus, and temperature with respect to T_{tr} to emphasise the continuous change of the precursor softening above T_{tr} with composition, from a gradual decrease of BaTiO_3 to a sharp decay in SrTiO_3 .

For numerical fits, the compliances S_{ij} are split into the background compliance S_{ij}^{bg} and the precursor softening ΔS due to the phase transition. The temperature dependence of S^{bg} is approximated to be linear with saturation below a temperature Θ , that can be described in terms of the quantum saturation expression [67]

$$S_{bg} = S_0 + S_1 \coth(\Theta/T). \quad (6)$$

The precursor softening is

$$\Delta S_{\text{power}} = A(T/T_C - 1)^{-\kappa} \quad (7)$$

for the power law and

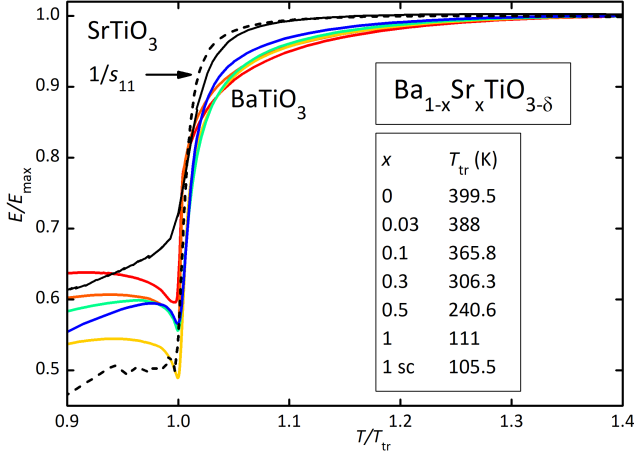


FIG. 3. Young's moduli of $\text{Ba}_{1-x}\text{Sr}_x\text{TiO}_{3-\delta}$ normalized to their maximum on a T/T_{tr} scale with T_{tr} listed in the insert.

$$\Delta S_{VF} = B(1 - \exp[-E_a/(T - T_{VF})]) \quad (8)$$

for the Vogel-Fulcher approach. If all the compliances S_{ij} have the same temperature dependences of background and precursor components, though with different amplitudes, the fitting expression

$$E/E_0 = 1/S = 1/(S_0 + S_1 \coth(\Theta/T) + \Delta S) \quad (9)$$

is valid for both ceramics and single crystal.

Figure 4 shows fits of the normalized moduli of ceramic BaTiO_3 and single crystal SrTiO_3 with Eq. (9) and both Eqs. (7) and (8) and the parameters indicated in the legends. The dashed lines represent the background S_{bg} , which is obtained setting A or $B = 0$. For the case of the power law in BaTiO_3 , S_{bg} is out of scale: from 1.18 at 760 K to 1.38 at 400 K. Similar fits are obtained for the intermediate compositions.

Figure 5 shows the dependence of the parameters κ, A and E_a, B on composition x . The error bars indicate the parameters regions where $\chi^2/\chi_{\min}^2 \leq 2$. The error bars for the VF parameters are quite large, because the VF expression tends to $B \times E_a/(T - T_{VF})$ for small $E_a/(T - T_{VF})$, and therefore the fit does not change reducing E_a below a certain value. This situation occurs at all compositions, where a decrease but no definite minimum of χ^2 is obtained decreasing E_a and simultaneously increasing B , except for SrTiO_3 , where a clear minimum is found for $E_a = 0.50^{+0.05}_{-0.09}$ K.

The power law dependence is well demonstrated with exponent $\kappa \simeq 0.2$ for BaTiO_3 increasing continuously to 1.5 for SrTiO_3 . The activation energy E_a decreases from ~ 3 K to 0.50 K. Simultaneously, the amplitudes A and B decrease continuously. For both parameters a plateau for intermediate compositions near $x = 0.4$ appears to occur.

To better show the close adherence of the precursor softening of BaTiO_3 and SrTiO_3 to a power law, Fig. 6 presents double logarithmic plots versus reduced temperature of the

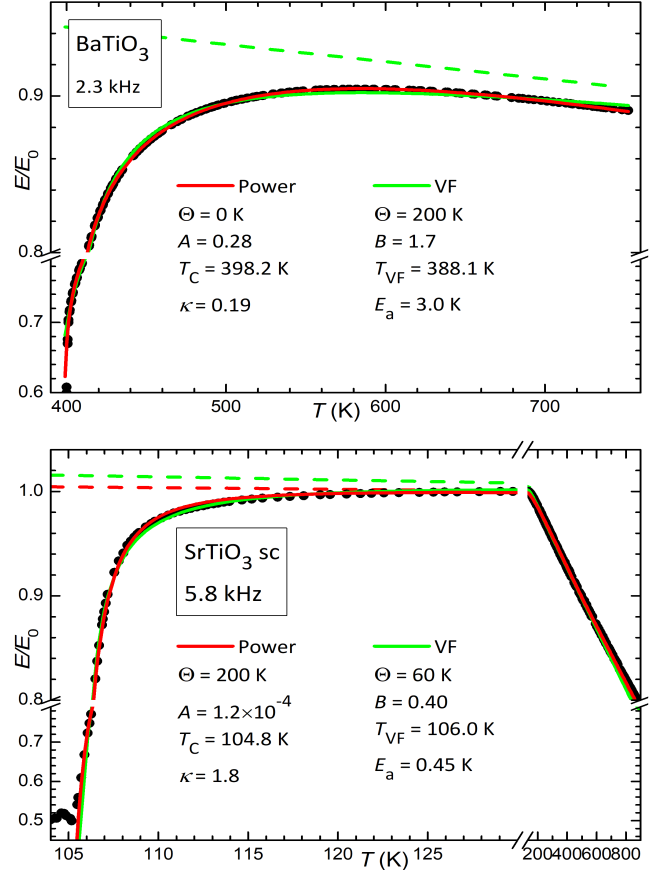


FIG. 4. Fits of the normalized Young's moduli of BaTiO_3 and SrTiO_3 with Eqs. (9-8) for the power law and Vogel-Fulcher analyses and the parameters indicated in the legends. The dashed lines represent S_{bg} , obtained setting A or $B = 0$. For the case of the power law in BaTiO_3 , S_{bg} is out of scale: from 1.18 at 760 K to 1.38 at 400 K.

precursor softening, $\Delta S_{\text{power}} = (E/E_0)^{-1} - S_{bg}$, where S_{bg} is obtained from the fits setting $A = 0$. The exponents in the legends are obtained from the linear fits of the log-log plots and coincide with the κ parameters of the corresponding fits. The deviations from the power law at small reduced temperature depend largely on the first order step of the modulus at the transition point between the cubic and tetragonal phase and the very large softening regime. Particularly impressive is the fact that BaTiO_3 closely follows a power law to $T_C + 360$ K, the maximum temperature measured.

V. DISCUSSION

The focus of the present analysis is the precursor softening in $\text{Ba}_x\text{Sr}_{1-x}\text{TiO}_3$ beyond the classical critical regime, from few Kelvin above T_{tr} up to the highest temperature reached in our experiments. The major finding is that even in this huge temperature range it is possible to describe the temperature dependence of the elastic moduli in terms of a power law with exponent in line with predictions from models of an-

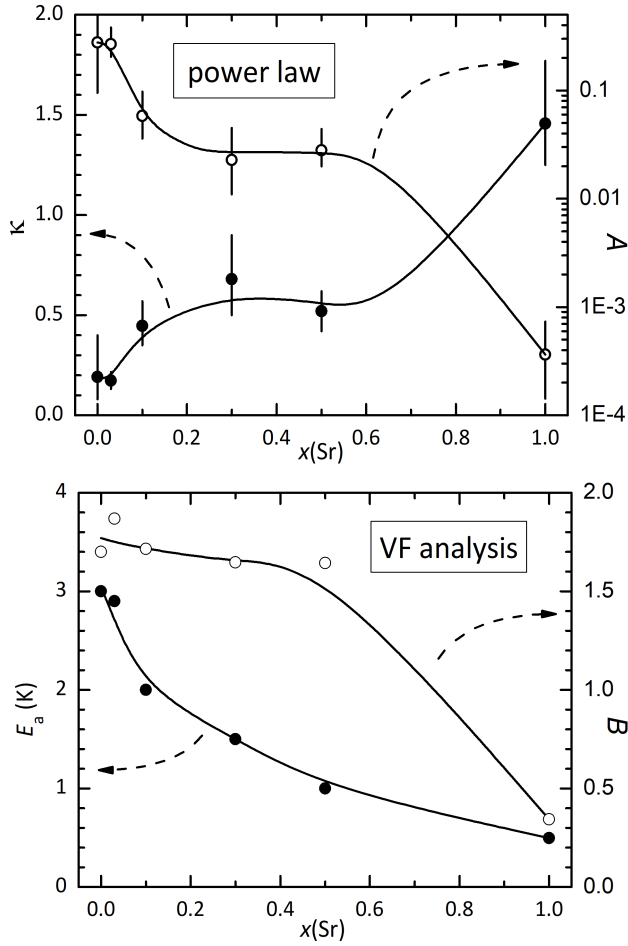


FIG. 5. Variation of power law and Vogel-Fulcher fit parameters with composition x . The continuous lines are guides for the eye.

harmonic phonon softening or, with somewhat less success, with a Vogel-Fulcher expression. In both cases the fitting parameter evolve with composition as expected from increasing order-disorder character from SrTiO₃ to BaTiO₃.

The power-law and Vogel-Fulcher elastic softening theoretically converge for small Vogel-Fulcher energies with power-law exponents near unity. We can therefore define a rather strict "displacive limit" when the Vogel-Fulcher energy vanishes, which is nearly the case for SrTiO₃. In all other compounds we observe small but finite values of E_a which indicate some weak contributions of structural disorder. This component increases with increasing Ba content, but always remains below the behaviour of a typical order-disorder system. On the other hand, the power law fits show that the anharmonic phonons coupled with the elastic moduli change their character, in particular their dimensionality in the model in Ref. [2]. If a single branch flattens, the exponent κ becomes 1.5. If two orthogonal branches flatten while the third remains relatively steep, we expect $\kappa = 1$. Finally, if three orthogonal branches flatten, the expected value is $\kappa = 0.5$. The experimental observations are surprisingly close to these values for

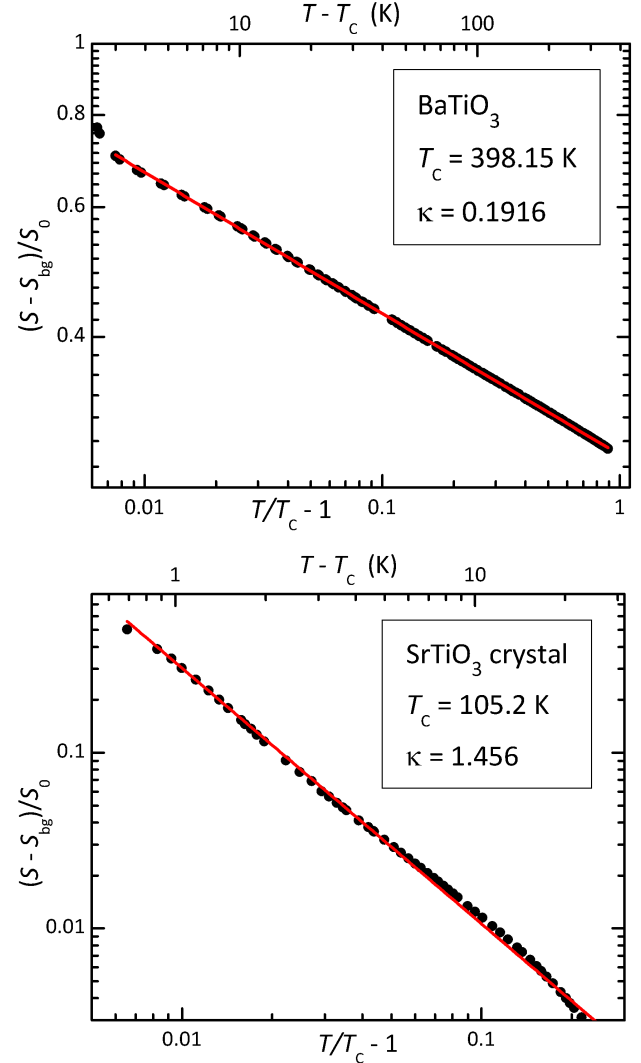


FIG. 6. Double logarithmic plots of the precursor softening vs reduced temperature of BaTiO₃ and SrTiO₃, $\Delta S_{\text{power}} = (E/E_0)^{-1} - S_{bg}$, where S_{bg} is obtained from the fits setting $A = 0$. The real temperatures are shown in the upper scales.

SrTiO₃ while somewhat exceed the lower limit for BaTiO₃. Simultaneously we observe that the precursor temperature interval is smallest for SrTiO₃ while it remains extremely large for Ba-rich materials with significant softening at least up to 800 K. Similar exponents, but smaller precursor temperature intervals, were previously observed in isostructural KMnF₃ and $\text{KMn}_x\text{Ca}_{1-x}\text{F}_3$ [29, 68, 69] with values of κ ranging between 0.4 and 1. In $\text{PbSc}_{0.5}\text{Ta}_{0.5}\text{O}_3$ (PST) the exponent is near 0.5 [70] with a smaller precursor interval, while $\sim 1/3$ has recently been found for structural fluctuations in cuprate superconductors [43].

An intriguing consequence of the precursor softening and the ensuing potential heterogeneity in SrTiO₃ was discussed in [71] where a strong coupling with the local carrier concentration was described. It was found that even very small

amounts of dopants can stabilize the soft phonon branches. This is linked to the formation of polar nano-regions, which grow in size with decreasing temperature. Such nano-regions would modify the precursor exponent κ and would also lead to an increase of the VF activation energy. More generally [72] precursor effects are a key to understand the fundamental aspects of the structural phase transitions in perovskite structures which are unrelated to some traditional concepts of the structural tolerance factors and small-cell DFT calculations. The mixing of transition mechanisms is most obvious in BaTiO_3 and related materials. Their phase transitions are accompanied by optic mode softening which remains incomplete near T_{tr} due to the first order nature of the phase transition [73]. Simultaneously local probe measurements show an order-disorder behaviour [4, 52, 74]. The coexistence of both, order/disorder and displacive mechanisms, has been widely discussed [75, 76]. Migoni *et al.* [77] pointed out that the most important ingredient of modelling of the soft mode activities is the directional anisotropic core-shell coupling at the oxygen ion lattice site, which is nonlinear with respect to the transition metal and harmonic with respect to the A-site cation. This mirrors our observation that dimensionality and hence the intrinsic anisotropy of the softening process play a major role in the precursor effects of $\text{Ba}_{1-x}\text{Sr}_x\text{TiO}_3$. We relate the difference between the end members for both model fits to the different phonon dispersions as calculated by Busmann-Holder and co-workers [72], who found that the transverse acoustic zone boundary TA mode couples strongly to the optic mode at finite momentum. The TA mode is presumed to be the origin of finite size precursors and polar nanoregions. This mode is less temperature dependent than the soft TO mode, which softens more strongly in BaTiO_3 and less in SrTiO_3 . A crossing of the zone boundary and the zone centre mode with decreasing temperature occurs in BaTiO_3 but not in SrTiO_3 . The avoided mode crossing induces precursor dynamics at small momenta which are less developed in BaTiO_3 where the optic mode softens over the full momentum space. These authors already argued that the softening of the optic mode in BaTiO_3 for all momenta is reminiscent of the breather type excitation and a signature for the formation of polar nanoregions far above the actual phase transition, which mirrors our findings.

There appears no definite onset for the softening, because all compositions can be well fitted up to $4T_{\text{C}}$ or the highest temperature reached experimentally with a power law or VF expression, without a characteristic temperature. This was expected for the displacive transition of non-polar SrTiO_3 , but not for Ba-rich compositions and especially BaTiO_3 , where characteristic temperatures have been identified below which polar nanoclusters start forming, i.e. the Burns temperature $T_d \sim 550\text{--}590\text{ K}$ and $T^* \sim 500\text{ K}$ [78–83]. The experimental signatures of such onsets or crossover temperatures are deviations from linearity in the temperature dependence of the refraction index [78], of thermal expansion [80], of the elastic constants at very high frequency [81], or maximum in the elastic moduli at MHz frequencies [83], bursts of Acoustic Emission [79], and a subtle change in the exponent of the power law describing the Second Harmonic Generation [82]. Below T_d

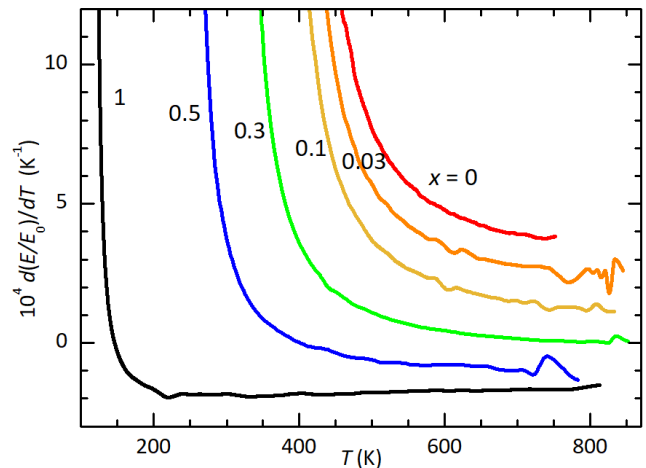


FIG. 7. Temperature derivatives of the Young's moduli of $\text{Ba}_x\text{Sr}_{1-x}\text{TiO}_3$. For clarity the curves are shifted of 10^{-4} K^{-1} with respect to each other. The larger noise at the highest temperature in some curves is due to the fact that the measurements were very fast there (up to 7 K/min) in order to limit possible losses of O in high vacuum.

nanoregions with static average displacements have been observed to develop with STEM and Raman spectroscopy [84].

Our data and their analyses do not show any evidence of such characteristic temperatures up to the highest we reached. This is better seen in the temperature derivatives of the moduli, shown in Fig. 7, where there is no evidence of inflections of the $E(T)$ curves.

It appears possible that in $\text{Ba}_x\text{Sr}_{1-x}\text{TiO}_3$ (away from the relaxor compositions $x \sim 0.15$) the measured T_d may define the onset temperature range below which some precursor phenomena were detected, while such temperatures seem not to appear in elastic softening. There are many theoretical models to account for elastic precursor softening, including the appearance of polar nano-clusters, local intrinsic correlations of precursor displacements [85] etc. while, surprisingly, the quantitative temperature evolution of the excess softening follows simple power-law (or Vogel-Fulcher) dynamics. This observation also reveals that the bare elastic moduli (when the precursor softening is eliminated) are much bigger than measured even at very high temperatures. As an example, with power-law fitting, at the highest temperature 750 K reached in BaTiO_3 the bare elastic modulus is 34% larger than the experimentally observed value, and at 840 K the bare modulus of $\text{Ba}_{0.03}\text{Sr}_{0.97}\text{TiO}_3$ is 22% larger than the experimental value, so that BaTiO_3 would be even stiffer than SrTiO_3 in the absence of precursor softening.

VI. CONCLUSIONS

Elastic precursor effects are common in ferroelastic materials. An increasing number of publications report such effects although with little or no numerical analysis of the observed

temperature dependencies. We proposed two frameworks to analyse such effects by power law dependence and a Vogel-Fulcher dynamics. It is very likely that these approaches are indeed universal. We urge the community to analyse such effects in the paraelastic phase and/or paraelectric phase because several applications may be based not only on domain boundaries [86] but also on the dynamic effects in the high symmetry phase. To demonstrate this behaviour, we reported in this paper the precursor softening of two prototypical materials and their mixed crystals. We found a smooth crossover between a displacive and a (partially) order-disorder system so that the precursor dynamics can be tailored according to specific applications. We presume that other structural imperfections, such as oxygen defects, will contribute similarly to local structural disorder and enhance the BaTiO₃-type elastic softening with extremely wide temperature intervals and low

exponents κ .

ACKNOWLEDGMENTS

The authors thank Vincenzo Buscaglia (CNR-ICMATE) for supplying the ceramic samples of SrTiO₃ and Ba_{0.5}Sr_{0.5}TiO₃ and Massimiliano Paolo Latino (CNR-ISM) for his technical assistance. EKHS is grateful to EPSRC for financial support (EP/P024904/1). PSSJ and MV are grateful to the Brazilian funding agencies for financial support: São Paulo State Research Foundation FAPESP (grants #2012/08457-7 and #2022/08030-5) and National Council for Scientific and Technological Development (CNPq) grant #304144/2021-5.

-
- [1] Ekhard K.H. Salje. Ferroelastic materials. *Annual Review of Materials Research*, 42(1):265–283, 2012.
- [2] Michael A. Carpenter and Ekhard K. H. Salje. Elastic anomalies in minerals due to structural phase transitions. *Eur. J. Mineral.*, 10(4):693–812, 1998.
- [3] Yoshihiro Ishibashi, Kazuhiro Hara, and Akitatsu Sawada. The ferroelastic transition in some scheelite-type crystals. *Physica BC*, 150(1):258–264, 1988.
- [4] T. Ishidate and S. Sasaki. Elastic Anomaly and Phase Transition of BaTiO₃. *Phys. Rev. Lett.*, 62:67–70, 1989.
- [5] Gilles Errandonea. Elastic and mechanical studies of the transition in LaP₅O₁₄: A continuous ferroelastic transition with a classical Landau-type behavior. *Phys. Rev. B*, 21:5221–5236, 1980.
- [6] A. Bussmann-Holder, H. Beige, and G. Völkel. Precursor effects, broken local symmetry, and coexistence of order-disorder and displacive dynamics in perovskite ferroelectrics. *Phys. Rev. B*, 79:184111, 2009.
- [7] A. V. Kityk, W. Schranz, P. Sondergeld, D. Havlik, E. K. H. Salje, and J. F. Scott. Low-frequency superelasticity and nonlinear elastic behavior of SrTiO₃ crystals. *Phys. Rev. B*, 61:946–956, 2000.
- [8] F. Cordero, F. Craciun, F. Trequattrini, and C. Galassi. Piezoelectric softening in ferroelectrics: ferroelectric versus antiferroelectric PbZr_{1-x}Ti_xO₃. *Phys. Rev. B*, 93:174111, 2016.
- [9] F. Cordero. Piezoelectricity from Elastic and Dielectric Measurements on Unpoled Ferroelectrics. *Mater. Res.*, 21(suppl.2):e20170852, 2018.
- [10] E. K. H. Salje, H. Zhang, H. Idrissi, D. Schryvers, M. A. Carpenter, X. Moya, and A. Planes. Mechanical resonance of the austenite/martensite interface and the pinning of the martensitic microstructures by dislocations in Cu_{74.08}Al_{23.13}Be_{2.79}. *Phys. Rev. B*, 80:134114, 2009.
- [11] Anna N. Morozovska, Eugene A. Eliseev, G. S. Svechnikov, and Sergei V. Kalinin. Mesoscopic mechanism of the domain wall interaction with elastic defects in uniaxial ferroelectrics. *J. Appl. Phys.*, 113(18):187203, 2013.
- [12] Xiaomei He, Suzhi Li, Xiangdong Ding, Jun Sun, Sergey Kustov, and Ekhard K.H. Salje. Internal friction in complex ferroelastic twin patterns. *Acta Materialia*, 228:117787, 2022.
- [13] W. T. Lee, E. K. H. Salje, L. Goncalves-Ferreira, M. Darakchiev, and U. Bismayer. Intrinsic activation energy for twin-wall motion in the ferroelastic perovskite CaTiO₃. *Phys. Rev. B*, 73:214110, 2006.
- [14] W. T. Lee, E. K. H. Salje, and U. Bismayer. Influence of point defects on the distribution of twin wall widths. *Phys. Rev. B*, 72:104116, 2005.
- [15] Liliana Goncalves-Ferreira, Simon A. T. Redfern, Emilio Artacho, Ekhard Salje, and William T. Lee. Trapping of oxygen vacancies in the twin walls of perovskite. *Phys. Rev. B*, 81:024109, 2010.
- [16] Deniz Ertas and David R. Nelson. Irreversibility, mechanical entanglement and thermal melting in superconducting vortex crystals with point impurities. *Physica C: Supercond.*, 272(1):79–86, 1996.
- [17] Thierry Giamarchi and Pierre Le Doussal. Elastic theory of flux lattices in the presence of weak disorder. *Phys. Rev. B*, 52:1242–1270, 1995.
- [18] Jutta Chrosch and Ekhard K. H. Salje. Temperature dependence of the domain wall width in LaAlO₃. *J. Appl. Phys.*, 85(2):722–727, 1999.
- [19] B. Wruck, E. K. H. Salje, M. Zhang, T. Abraham, and U. Bismayer. On the thickness of ferroelastic twin walls in lead phosphate Pb₃(PO₄)₂ an X-ray diffraction study. *Phase Transit.*, 48(1-3):135–148, 1994.
- [20] Richard J. Harrison and Simon A.T. Redfern. The influence of transformation twins on the seismic-frequency elastic and anelastic properties of perovskite: dynamical mechanical analysis of single crystal LaAlO₃. *Phys. Earth Planet. Inter.*, 134(3):253–272, 2002.
- [21] H. Küpfer, A. A. Zhukov, A. Will, W. Jahn, R. Meier-Hirmer, Th. Wolf, V. I. Voronkova, M. Kläser, and K. Saito. Anisotropy in the irreversible behavior of pointlike defects and twins in YBa₂Cu₃O_{7- δ} single crystals with a peak effect. *Phys. Rev. B*, 54:644–655, 1996.
- [22] Ekhard K. H. Salje. Elastic softening of zircon by radiation damage. *Appl. Phys. Lett.*, 89(13):131902, 2006.
- [23] Ekhard K.H. Salje, Douglas J. Safarik, Jason C. Lashley, Lee A. Groat, and Ulli Bismayer. Elastic softening of metamict titanite CaTiSiO₅: Radiation damage and annealing. *Am. Mineral.*, 96(8-9):1254–1261, 2011.
- [24] X. G. Zhao, G. M. Dalpian, Z. Wang, and A. Zunger. Polymorphous nature of cubic halide perovskites. *Phys. Rev. B*, 101:155137, 2020.

- [25] Oktay Aktas, Moussa Kangama, Gan Linyu, Gustau Catalan, Xiangdong Ding, Alex Zunger, and Ekhard K. H. Salje. Piezoelectricity in nominally centrosymmetric phases. *Phys. Rev. Research*, 3:043221, 2021.
- [26] Oktay Aktas, Ekhard K. H. Salje, Sam Crossley, Giulio I. Lampronti, Roger W. Whatmore, Neil D. Mathur, and Michael A. Carpenter. Ferroelectric precursor behavior in $\text{PbSc}_{0.5}\text{Ta}_{0.5}\text{O}_3$ detected by field-induced resonant piezoelectric spectroscopy. *Phys. Rev. B*, 88:174112, 2013.
- [27] O. Aktas, M. Kangama, G. Linyu, X. Ding, M.A. Carpenter, and E.K.H. Salje. Probing the dynamic response of ferroelectric and ferroelastic materials by simultaneous detection of elastic and piezoelectric properties. *J. Alloys Compd.*, 903:163857, 2022.
- [28] Xin-Gang Zhao, Oleksandr I. Malyi, Simon J. L. Billinge, and Alex Zunger. Intrinsic local symmetry breaking in nominally cubic paraelectric BaTiO_3 . *Phys. Rev. B*, 105:224108, 2022.
- [29] Wenwu Cao and Gerhard R. Barsch. Elastic constants of KMnF_3 as functions of temperature and pressure. *Phys. Rev. B*, 38:7947–7958, 1988.
- [30] E. Pytte. Soft-Mode Damping and Ultrasonic Attenuation at a Structural Phase Transition. *Phys. Rev. B*, 1:924–930, 1970.
- [31] E Pytte. *Structural Phase Transitions and Soft Modes*, page 133. Universitetsforlaget, Oslo, 1971.
- [32] J. D. Axe and G. Shirane. Study of the α - β Quartz Phase Transformation by Inelastic Neutron Scattering. *Phys. Rev. B*, 1:342–348, 1970.
- [33] U. T. Höchli. Elastic constants and soft optical modes in gadolinium molybdate. *Phys. Rev. B*, 6:1814–1823, 1972.
- [34] Walther Rehwald. The study of structural phase transitions by means of ultrasonic experiments. *Adv. Phys.*, 22(6):721–755, 1973.
- [35] H. Z. Cummins. Brillouin scattering spectroscopy of ferroelectric and ferroelastic phase transitions. *Philos. Trans. Royal Soc. A*, 293:393–405, 1979.
- [36] B Lüthi and W Rehwald. Ultrasonic studies near structural phase transitions. In *Structural Phase Transitions I*, pages 131–184. Springer, 1981.
- [37] W. Yao, H. Z. Cummins, and R. H. Bruce. Acoustic anomalies in terbium molybdate near the improper ferroelastic-ferroelectric phase transition. *Phys. Rev. B*, 24:424–444, 1981.
- [38] J. O. Fossum. A phenomenological analysis of ultrasound near phase transitions. *J. Phys. C Solid State Phys.*, 18(29):5531, 1985.
- [39] E. Salje and K. Parlinski. Microstructures in high T_c superconductors. *Supercond. Sci. Technol.*, 4:93, 1991.
- [40] S. Marais, V. Heine, C. Nex, and E. Salje. Phenomena due to strain coupling in phase transitions. *Phys. Rev. Lett.*, 66:2480, 1991.
- [41] P. Lloveras, T. Castán, M. Porta, A. Planes, and A. Saxena. Influence of Elastic Anisotropy on Structural Nanoscale Textures. *Phys. Rev. Lett.*, 100:165707, 2008.
- [42] Yong Ni and Armen G. Khachatryan. From chessboard tweed to chessboard nanowire structure during pseudospinodal decomposition. *Nat. Mater.*, 8:410, 2009.
- [43] D. Pelc, R. J. Spieker, Z. W. Anderson, M. J. Krogstad, N. Biniskos, N. G. Bielinski, B. Yu, T. Sasagawa, L. Chauviere, P. Dosanjh, R. Liang, D. A. Bonn, A. Damascelli, S. Chi, Y. Liu, R. Osborn, and M. Greven. Unconventional short-range structural fluctuations in cuprate superconductors. *Sci. Rep.*, 12:20483, 2022.
- [44] J. F. Scott and S. P. S. Porto. Longitudinal and Transverse Optical Lattice Vibrations in Quartz. *Phys. Rev.*, 161:903, 1967.
- [45] Xiaofei Wang, Ekhard K. H. Salje, Jun Sun, and Xiangdong Ding. Glassy behavior and dynamic tweed in defect-free multiferroics. *Appl. Phys. Lett.*, 112(1):012901, 2018.
- [46] Ekhard K. H. Salje, Michael A. Carpenter, Guillaume F. Nataf, Gunnar Picht, Kyle Webber, Jeevaka Weerasinghe, S. Lisenkov, and L. Bellaiche. Elastic excitations in BaTiO_3 single crystals and ceramics: Mobile domain boundaries and polar nanoregions observed by resonant ultrasonic spectroscopy. *Phys. Rev. B*, 87:014106, 2013.
- [47] M.A. Carpenter, J.F.J Bryson, G. Catalan, S.J. Zhang, and N.J. Donnelly. Elastic and anelastic relaxations in the relaxor ferroelectric $\text{PbMg}_{1/3}\text{Nb}_{2/3}\text{O}_3$: II. Strain-order parameter coupling and dynamic softening mechanisms. *J. Phys.: Condens. Matter*, 24(4):045902, 2011.
- [48] E. K. H. Salje, X. Ding, and O. Aktas. Domain glass. *Phys. Stat. Sol. (b)*, 251(10):2061–2066, 2014.
- [49] R. I. Thomson, T. Chatterji, and M. A. Carpenter. CoF_2 : a model system for magnetoelastic coupling and elastic softening mechanisms associated with paramagnetic \leftrightarrow antiferromagnetic phase transitions. *J. Phys.: Condens. Matter*, 26:146001, 2022.
- [50] EKH Salje, MC Gallardo, J Jiménez, FJ Romero, and J Del Cerro. The cubic-tetragonal phase transition in strontium titanate: excess specific heat measurements and evidence for a near-tricritical, mean field type transition mechanism. *J. Phys.: Condens. Matter*, 10(25):5535, 1998.
- [51] Bo štjan Zalar, Valentin V. Laguta, and Robert Blinc. NMR Evidence for the Coexistence of Order-Disorder and Displacive Components in Barium Titanate. *Phys. Rev. Lett.*, 90:037601, 2003.
- [52] B. Zalar, A. Lebar, J. Seliger, R. Blinc, V. V. Laguta, and M. Itoh. NMR study of disorder in BaTiO_3 and SrTiO_3 . *Phys. Rev. B*, 71:064107, 2005.
- [53] I. B. Bersuker. Jahn-Teller and Pseudo-Jahn-Teller Effects: From Particular Features to General Tools in Exploring Molecular and Solid State Properties. *Chem. Rev.*, 121:1463, 2021.
- [54] Sergey Kustov, Iulia Liubimova, and Ekhard K. H. Salje. Domain Dynamics in Quantum-Paraelectric SrTiO_3 . *Phys. Rev. Lett.*, 124:016801, 2020.
- [55] A. Migliori, J. L. Sarrao, W. M. Visscher, T. M. Bell, M. Lei, Z. Fisk, and R. G. Leisure. Resonant ultrasound spectroscopic techniques for measurement of the elastic moduli of solids. *Phys. B: Condens. Matter*, 183(1-2):1–24, 1993.
- [56] S. Aubry. A unified approach to the interpretation of displacive and order-disorder systems. I. Thermodynamical aspect. *J. Chem. Phys.*, 62:3217, 1975.
- [57] S. Aubry. A unified approach to the interpretation of displacive and order-disorder systems. II. Displacive systems. *J. Chem. Phys.*, 64:3392, 1976.
- [58] F Cordero, F Trequattrini, DAB Quiroga, and PS Silva Jr. Hopping and clustering of oxygen vacancies in $\text{BaTiO}_{3-\delta}$ and the influence of the off-centred Ti atoms. *J. Alloys Compd.*, 874:159753, 2021.
- [59] F. Cordero, L. Dalla Bella, F. Corvasce, P. M. Latino, and A. Morbidini. An insert for anelastic spectroscopy measurements from 80 K to 1100 K. *Meas. Sci. Technol.*, 20:015702, 2009.
- [60] A.S. Nowick and B.S. Berry. *Anelastic Relaxation in Crystalline Solids*. Materials Science and Technology Series. Academic Press, 1972.
- [61] V. V. Lemanov, E. P. Smirnova, P. P. Syrnikov, and E. A. Tarakanov. Phase transitions and glasslike behavior in $\text{Sr}_{1-x}\text{Ba}_x\text{TiO}_3$. *Phys. Rev. B*, 54:3151–3157, 1996.

- [62] Ekhard Salje, J. Koppensteiner, Wilfried Schranz, and Fritsch E. Elastic instabilities in dry, mesoporous minerals and their relevance to geological applications. *Mineralogical Magazine*, 72:341, 2010.
- [63] Martin L. Dunn. Effects of grain shape anisotropy, porosity, and microcracks on the elastic and dielectric constants of polycrystalline piezoelectric ceramics. *J. Appl. Phys.*, 78(3):1533–1541, 1995.
- [64] F. Cordero. Quantitative evaluation of the piezoelectric response of unpoled ferroelectric ceramics from elastic and dielectric measurements: Tetragonal BaTiO₃. *J. Appl. Phys.*, 123(9):094103, 2018.
- [65] Don Berlincourt and Hans Jaffe. Elastic and Piezoelectric Coefficients of Single-Crystal Barium Titanate. *Phys. Rev.*, 111:143–148, 1958.
- [66] Michael A Carpenter. Elastic anomalies accompanying phase transitions in (Ca,Sr)TiO₃ perovskites: Part II. Calibration for the effects of composition and pressure. *Am. Mineral.*, 92(2-3):328–343, 2007.
- [67] E.K.H. Salje, B. Wruck, and H. Thomas. Order-parameter saturation and low-temperature extension of Landau theory. *Z. Phys. B - Condensed Matter*, 82:399, 1991.
- [68] W. Schranz, P. Sonderegeld, A. V. Kityk, and E. K. H. Salje. Dynamic elastic response of KMn_{1-x}Ca_xF₃: Elastic softening and domain freezing. *Phys. Rev. B*, 80:094110, 2009.
- [69] Ekhard K H Salje and Huali Zhang. Domain boundary pinning and elastic softening in KMnF₃ and KMn_{1-x}Ca_xF₃. *J. Phys.: Condens. Matter*, 21(3):035901, 2009.
- [70] G. Linyu, F. J. Romero, V. Franco, J. M. Martin-Olalla, M. C. Gallardo, E. H. Salje, Y. Zhou, and O. Aktas. Correlations between elastic, calorimetric, and polar properties of ferroelectric PbSc_{0.5}Ta_{0.5}O₃ (PST). *Appl. Phys. Lett.*, 115:161904, 2019.
- [71] Annette Bussmann-Holder, Hugo Keller, Arndt Simon, Gustav Bihlmayer, Krystian Roleder, and Krzysztof Szot. Unconventional Co-Existence of Insulating Nano-Regions and Conducting Filaments in Reduced SrTiO₃: Mode Softening, Local Piezoelectricity, and Metallicity. *Crystals*, 10(6), 2020.
- [72] A. Bussmann-Holder, K. Roleder, and J. H. Ko. What makes the difference in perovskite titanates? *J. Phys. Chem. Sol.*, 117:148, 2018.
- [73] J. Harada, J. D. Axe, and G. Shirane. Neutron-Scattering Study of Soft Modes in Cubic BaTiO₃. *Phys. Rev. B*, 4:155–162, 1971.
- [74] R. Z. Tai, K. Namikawa, A. Sawada, M. Kishimoto, M. Tanaka, P. Lu, K. Nagashima, H. Maruyama, and M. Ando. Picosecond View of Microscopic-Scale Polarization Clusters in Paraelectric BaTiO₃. *Phys. Rev. Lett.*, 93:087601, 2004.
- [75] V. L. Kraizman, A. A. Novakovich, R. V. Vedrinskii, and V. A. Timoshevskii. Formation of the pre-edge structure and dramatic polarization dependence of Ti K NEXAFS in PbTiO₃ crystals. *Phys. B: Condens. Matter*, 208-209:35–36, 1995.
- [76] M. Stachiotti, A. Dobry, R. Migoni, and A. Bussmann-Holder. Crossover from a displacive to an order-disorder transition in the nonlinear-polarizability model. *Phys. Rev. B*, 47:2473–2479, 1993.
- [77] R. Migoni, H. Bilz, and D. Bäuerle. Origin of raman scattering and ferroelectricity in oxidic perovskites. *Phys. Rev. Lett.*, 37:1155–1158, 1976.
- [78] G. Burns and F. H. Dacol. Polarization in the cubic phase of BaTiO₃. *Solid State Commun.*, 42:9, 1982.
- [79] E. Dul'kin, J. Petzelt, S. Kamba, E. Mojaev, and M. Roth. Relaxor-like behavior of BaTiO₃ crystals from acoustic emission study. *Appl. Phys. Lett.*, 97:032903, 2010.
- [80] V. Mueller, L. Jäger, H. Beige, H. P. Abicht, and T. Müller. Thermal expansion in the Burns-phase of barium titanate stannate. *Solid State Commun.*, 129:757, 2004.
- [81] S. Kojima and S. Tsukada. Micro-Brillouin Scattering of Relaxor Ferroelectrics with Perovskite Structure. *Ferroelectrics*, 405:32, 2010.
- [82] A. M. Pugachev, V. I. Kovalevskii, N. V. Surovtsev, S. Kojima, S. A. Prosandeev, I. P. Raevski, and S. I. Raevskaya. Broken Local Symmetry in Paraelectric BaTiO₃ Proved by Second Harmonic Generation. *Phys. Rev. Lett.*, 108:247601, 2012.
- [83] E. K. H. Salje, M. A. Carpenter, G. F. Nataf, G. Picht, K. Webber, J. Weerasinghe, S. Lisenkov, and L. Bellaiche. Elastic excitations in BaTiO₃ single crystals and ceramics: Mobile domain boundaries and polar nanoregions observed by resonant ultrasonic spectroscopy. *Phys. Rev. B*, 87:014106, 2013.
- [84] A. Bencan, E. Oveisi, Sina Hashemizadeh, Vignaswaran K. Veerapandiyam, Takuya Hoshina, Tadej Rojac, Marco Deluca, Goran Drazic, and Dragan Damjanovic. Atomic scale symmetry and polar nanoclusters in the paraelectric phase of ferroelectric materials. *Nat. Commun.*, 12:3509, 2021.
- [85] X. G. Zhao, O. I. Malyi, S. L. Billinge, and A. Zunger. Intrinsic local symmetry-breaking in nominally cubic paraelectric BaTiO₃. *Phys. Rev. B*, 105:224108, 2022.
- [86] G. F. Nataf, M. Guennou, J. M. Gregg, D. Meier, J. Hlinka, E. K. H. Salje, and J. Kreisel. Domain-wall engineering and topological defects in ferroelectric and ferroelastic materials. *Nat. Rev. Phys.*, 2:634, 2020.